



Improving the proton conductivity and water uptake of polybenzimidazole-based proton exchange nanocomposite membranes with TiO₂ and SiO₂ nanoparticles chemically modified surfaces

Hassan Namazi*, Hossein Ahmadi

Research Laboratory of Dendrimers and Nanopolymers, Faculty of Chemistry, University of Tabriz, 29 Bahman Blv, P.O. Box 5166616471, Tabriz, Iran

ARTICLE INFO

Article history:

Received 4 July 2010

Received in revised form 21 October 2010

Accepted 23 October 2010

Available online 4 November 2010

Keywords:

Polybenzimidazole

Proton exchange membrane

Modified nanoparticles

Sulfonated vinylbenzene

Vinylimidazole

ABSTRACT

Poly [2,2'-(*m*-pyrazolidene)-5,5'-bibenzimidazole] (PPBI) was synthesized from pyrazole-3,5-dicarboxylic acid and 3,3',4,4'-tetraaminobiphenyle (TAB) through polycondensation reaction in polyphosphoric acid (PPA) as reaction solvent. And polymer-grafted SiO₂ and TiO₂ nanoparticles were prepared through radical polymerization of 1-vinylimidazole and sulfonated vinylbenzene on the surface-vinylated nanoparticles. The polymer-grafted SiO₂ and TiO₂ nanoparticles were utilized as a functional additive to prepare PPBI/polymer-grafted SiO₂ and TiO₂ nanocomposite membranes. Imidazole and sulfonated vinylbenzene groups on the surface of modified nanoparticles forming linkages with PPBI chains, improved the compatibility between PPBI and nanoparticles, and enhanced the mechanical strength of the prepared nanocomposite membranes. The prepared nanocomposite membranes showed higher water uptake and acid doping levels comparing to PPBI. Also, after acid doping with phosphoric acid, nanocomposite membranes exhibited enhanced proton conductivity in comparison to the pristine PPBI and PPBI/un-modified SiO₂ and TiO₂ nanocomposite membranes. The enhancement in proton conductivity of nanocomposite membranes resulted from modified SiO₂ nanoparticles showed higher conductivity than modified TiO₂ nanoparticles. The above results indicated that the PPBI/modified SiO₂ and TiO₂ nanocomposite membranes could be utilized as proton exchange membranes for medium temperature fuel cells.

© 2010 Elsevier B.V. All rights reserved.

1. Introduction

In recent years, polymeric electrolytes based on hydrocarbons have been considered as an alternative for Nafion[®] membranes for high temperature polymer electrolyte fuel cells. Due to its high proton conductivity, Nafion[®] is an appropriate option to use in polymeric electrolyte fuel cells (PEFCs). The great proton conductivity of Nafion[®] membranes can be resulted from the presence of sulfonate groups in polymer structure and its adsorbed water. Because of water removal at temperatures above 80 °C, the proton conductivity of membranes decreases dramatically leading to a poor performance in fuel cells. In addition, the reason for the scientific enthusiasm for utilizing the fuel cells at elevated temperatures is that there is no need to use high-purity hydrogen at higher temperatures; besides, CO-existing in the H₂ fuel does not lead to the poisoning of electro-catalysts. Furthermore, at higher temperatures, the rate of red-ox reaction on electrolytes increases. On the other hand, there would be less need for the use of heat exchang-

ers [1–3]. Sulfonated polysulfone (PSF) [4], polyetheretherketone (PEEK) [5,6] and polybenzimidazoles (PBIs) [7–11] are among polymers which can be used as alternatives for Nafion in PEFCs.

Among polybenzimidazole derivatives, poly [2,2-5,5(*m*-phenylene)-bibenzimidazole] (PBI), which is also called commercial polybenzimidazole have been used as a membrane material in PEMFCs. Having high chemical as well as thermal resistance and proton conductivity, polybenzimidazoles are great options to be used in the fuel cells with function at elevated temperatures above 100 °C [12].

PBIs should have enough proton conductivity so that it could be used as proton exchange membranes in the fuel cells. To achieve this purpose, they are usually doped with a sufficient acid like H₃PO₄ to an appropriate doping level [13]. Nanocomposite membranes are a new group of membranes which contain nanoparticles such as SiO₂, TiO₂ and ZrO₂ and other compounds [14–21]. The introduction of nanoparticles into the membranes results in a considerable improvement in their features like mechanical properties, methanol permeability, but in some cases leads to a decrease in proton conductivity [22–24]. In order to overcome this problem, surface functionalized nanoparticles, which means various compounds with polar groups grafted chemically

* Corresponding author. Tel.: +98 411 3393121; fax: +98 411 3340191.
E-mail address: namazi@tabrizu.ac.ir (H. Namazi).

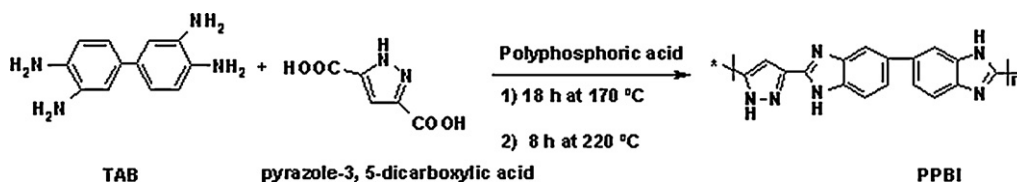


Fig. 1. The reaction of PPBI synthesis.

to the surface of the nanoparticles [25–28], were used. As mentioned before, the numerous research works were done concerning grafting various compounds on the SiO₂ and TiO₂ nanoparticles which used for different purposes. However, in this work, we have used monomer bearing functional groups like imidazole and sulfonated vinylbenzene which can improve the properties of proton conductive membranes. These monomers are polymerized on the surface of the nanoparticles and as a consequence, they can more affect the properties of the membranes than while one functional group is grafted onto the surface of the nanoparticles. In addition, the polymerization of the selected monomers such as vinylimidazole and sulfonated vinylbenzene on the surface of nanoparticle could cause more compatibility between nanoparticles and polymer matrix which finally improve the mechanical properties. In this work, nanocomposite membranes were prepared using various amounts of modified TiO₂ and SiO₂ nanoparticles and newly synthesized polybenzimidazole was depicted poly[2,2'-5,5'-(*m*-pyrazolidene)-bibenzimidazole] (PPBI). Modification of the mentioned nanoparticles was performed by radical polymerization of some vinyl monomers such as sulfonated styrene and vinylimidazole on the surface of the nanoparticles to which vinylic group was bounded covalently. Also, the effect of surface modification on the properties of the nanocomposite membranes such as proton conductivity, mechanical properties and water uptake were studied.

2. Experimental

2.1. Materials

3,3',4,4'-Tetraaminobiphenyl (TAB) was purchased from Fluka and purified by re-crystallization from hot water. Pyrazole-3,5-dicarboxylic acid, was purchased from Merck and used as received. SiO₂ and TiO₂ nanoparticles with diameters 13 and 24 nm respectively, were purchased from Degusa Company and used as received. Polyphosphoric acid, sodium vinylbenzene sulfonate and 1-vinylimidazole were purchased from Aldrich and were used without further treatment. *N,N*-Dimethylacetamide (DMAC) was purchased from Fluka and used as received. Tetrahydrofuran, trichlorovinylsilane, dimethylformamide (DMF) and dimethylsulfoxide (DMSO) were purchased from Aldrich Chemical and were distilled and dried before using.

2.2. Preparation of PPBI

PPBI was prepared using polycondensation reaction of equimolar of pyrazole-3,5-dicarboxylic acid and TAB monomers in polyphosphoric acid medium (Fig. 1). The monomers and polyphosphoric acid were added to a three-necked flask under argon atmosphere and stirred using mechanical overhead stirrer for 18 h at 170 °C and 8 h at 220 °C. After reaction completion, the viscose mixture was precipitated in water. It was then separated, neutralized with sodium hydroxide solution (10% w/w), washed thoroughly with water and dried in a vacuum oven for 24 h at 60 °C to obtain PPBI.

2.3. Modification of TiO₂ and SiO₂ nanoparticles

One gram of TiO₂ nanoparticles dried at 100 °C under vacuum was added into a 250 mL flask containing 100 mL of dry THF and 10 mL of dried trichlorovinylsilane (coupling agent) under argon atmosphere. The resulting dispersion was stirred at room temperature for 48 h. After completion of the reaction, the surface vinylated TiO₂ nanoparticles (TiO₂-vinylated) were separated and washed with THF several times to remove un-reacted trichlorovinylsilane. After drying of the resultant powder at 80 °C for 24 h under vacuum, 1.5 g of the dry vinylated TiO₂, 0.64 g 2,2'-azobis (isobutyronitrile) (AIBN) and 100 mL of dry DMF were added in to a 250 mL three-necked flask under argon atmosphere equipped with a condenser and stirred for 1 h at 75 °C and followed by drop-wise addition of 25 mL of vinylimidazole monomer to the mixture. At the end of the reaction, 50 mL of DMF was added to the mixture followed by stirring for 1 h at room temperature. After separation with centrifuge, the obtained powder (TiO₂-PVI) was washed several times with NaCl (0.1 M) solution and de-ionized water respectively, in order to remove the un-grafted polyvinylimidazole (PVI) chains from the surface.

In order to prepare TiO₂ nanoparticles modified by poly (sulfonated vinylbenzene) (TiO₂-PSV), 12.5 g of sulfonated vinylbenzene was dissolved in dry DMSO and then added to the mixture of 1.5 g of vinylated TiO₂ nanoparticles, 100 mL of DMSO and 1.0 g of AIBN at 75 °C under argon atmosphere while stirring. After 18 h, the obtained powder (TiO₂-PSV) was separated by centrifuge and washed several times with DMSO and ethanol and then dried at 60 °C under vacuum for 6 h. All of the above explanations were also applied to the chemical modification process of SiO₂ nanoparticles (Fig. 2).

2.4. Preparation of nanocomposite membranes and acid doping

Many different methods are used for the production of inorganic nanoparticles. For further manipulations of nanoparticles which usually exist as aggregates, they are dispersed in a liquid or solid medium. In this work the ultrasonic waves were used for dispersing the nanoparticles in polymeric solution for 1 h at 80 °C.

Nanocomposite membranes were prepared using PPBI and various amounts (5, 10 and 15% w/w) of both modified and un-modified nanoparticles by casting method from DMSO solvent on glass plates with thicknesses of 40–60 μm. After casting, the membranes were immersed in de-ionized water and then dried for 5 h at 80 °C under vacuum. Subsequently, they were immersed in phosphoric acid (85% w/w) at 30 °C for 3 days in order to be doped. After washing with water, doped membranes were dried at 80 °C for 24 h under vacuum.

2.5. Characterization techniques

Prior to polymer characterization, all polymers were dried at 80 °C in vacuum to a constant weight. Fourier transform infrared (FTIR) spectra were obtained with Bruker Fourier Transform Spectrophotometer. ¹H NMR spectra were acquired on a Bruker Instrument at 400 MHz in DMSO-d₆. Thermogravimetric analy-

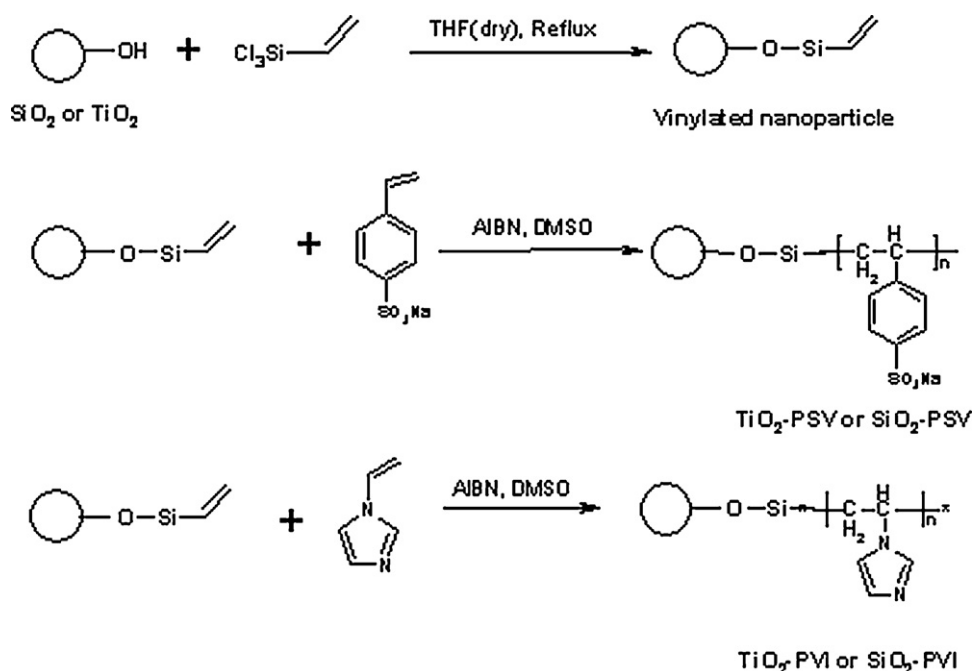


Fig. 2. The schematic of modification reactions of nanoparticles.

sis (TGA) spectra were recorded on a D.T.G. 60 AH Shimadzu Instruments at a heating rate of $10^\circ\text{C min}^{-1}$ in air atmosphere. Transmission electron microscopy (TEM) analysis was performed using a LEO 906 microscope with an 80 kV voltage.

The water uptake values of the prepared membranes were calculated using the following equation:

$$\text{Water uptake (\%)} = \frac{w_s - w_d}{w_d} \times 100$$

where w_s and w_d are membrane weights after and before dipping the dried membranes in distilled water for 24 h at 30°C , respectively. The membranes were dried at 100°C in vacuum for 3 h. The wet membranes were weighed after wiping with paper tissue in order to remove any surface moisture.

Acid doping levels (mole H_3PO_4 per PPBI repeating unit) were measured by dipping the membranes in an 85% phosphoric acid solution for 48 h. Membranes were weighed after washing with water and drying at 100°C under vacuum for 4 h.

Proton conductivity was measured by electrochemical impedance spectroscopy (EIS) using an EG&G Advanced Electrochemical System (PARSTAT 1263-Princeton Applied Research, USA) with a two electrode setup in the frequency range of 100 kHz–2 Hz (150 data points). The two electrodes were $1\text{ cm} \times 1\text{ cm}$ stainless steel plates mirror polished with emery type papers and washed

with de-ionized water and subsequently, with acetone before each experiment [29].

Studied membranes were sandwiched between the stainless steel electrodes with pressure applied by a clamp, counter and reference electrodes are both connected to one of the plates and the working electrode to the other plate.

The mechanical properties of the nanocomposite membranes were carried out by Universal Testing Machine (GOTECH, GT-TCS-208).

3. Results and discussion

3.1. ^1H NMR and FT-IR characterization

As seen in Fig. 3, the ^1H NMR spectrum of the synthesized polymer shows a singlet near 13.5 ppm for imidazole protons (N–H) and multiple signals in the region of 6–8 ppm for aromatic ones. The absence of absorbent peak related to amine group proton (N–H) in the area of 4.0–5.0 ppm and an absorbent related to amide group in the area of 10.3–10.6 ppm show the complete closure of imidazole rings during the polycondensation reaction.

In FT-IR characteristics of PPBI, the presence of absorbent bands in 800 cm^{-1} is related to the vibration of C–H bond of imidazole, a band in about 1300 cm^{-1} is related to the vibration of C–N

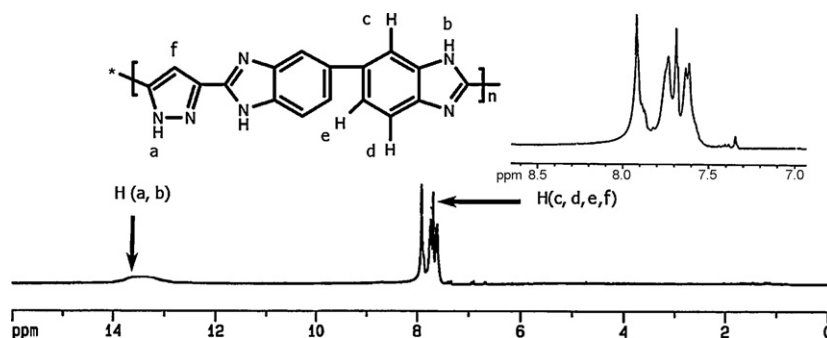


Fig. 3. The ^1H NMR spectrum of PPBI.

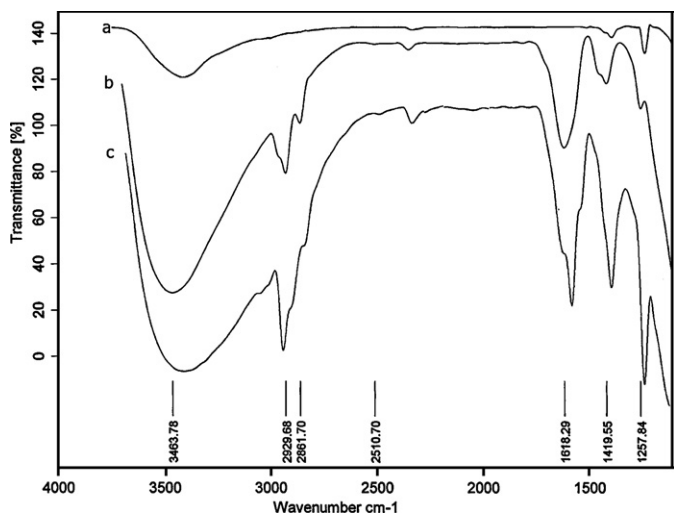


Fig. 4. FT-IR spectra of unmodified (a), PVI grafted (b) and PSV grafted (c) nanoparticles.

bond of imidazole, the absorbent band in 1450 cm^{-1} is related to C=N and C=C vibrations and bands in the area of 3400 cm^{-1} and 3140 cm^{-1} are related to N-H vibrations. All the above absorbent bands confirm the synthesis of PPBI. Furthermore, the absence of the absorbent band related to the carbonyl group in the vicinity of 1760 cm^{-1} can be confirmed as an evidence of the completion of cyclization reaction.

The FT-IR spectra of modified and un-modified SiO_2 nanoparticles are shown in Fig. 4(a and b, c), respectively. The presence of the absorbent bands in 3050 cm^{-1} and 3100 cm^{-1} can be related to aromatic C-H bonds and also the existence of bands in the area of 2950 cm^{-1} can be attributed to aliphatic C-H bonds. Also the peaks in 1619 and 1419 cm^{-1} can be due to C=C and C=N bonds. In

Fig. 4(c), the presence of the absorbent band in 1257 cm^{-1} is corresponded to S=O bond of the sulfonic acid group. These prove the existence of polymeric chains that are grafted onto the nanoparticle surface.

FT-IR spectra of the modified nanoparticles have been measured after complete washing and drying. To be sure of the chemical bonding of all chains (not physical) onto the particle surface, some un-modified nanoparticles were mixed with polymeric solutions of PVI and PSV and were stirred for 1 h. After filtration, the washing method used to wash the modified nanoparticles, was applied to the resulting powder as well. The FT-IR spectrum of the obtained powder did not show any absorbent bands related to PVI and PSV chains. The absorbent bands, which existed in the spectrum of modified nanoparticles, were not observed in this spectrum. So, it was indicated that the polymeric chains have been attached to the particles surface via covalent bonds.

3.2. Thermal analysis

Thermogravimetric analysis diagrams of both modified and un-modified nanoparticles are shown in Fig. 5. Weight loss in 85°C can be related to the release of physically absorbed water. In un-modified nanoparticles, the minor weight loss in elevated temperatures can be attributed to the loss of hydroxyl groups of the particle surface attached by covalent bonds. Weight loss in modified nanoparticles could be a result of thermal degradation of the polymeric chains grafted to the surface of the nanoparticles. Also, the weight loss in $230\text{--}300^\circ\text{C}$ was due to the thermal decomposition of the sulfonate groups in the grafted PSV chains [30].

Thermograms of PVI modified nanocomposite with 5, 10 and 15% of TiO_2 are shown in Fig. 6. As it is observed, the thermal properties of the nanocomposites prepared with various amounts of TiO_2 are almost similar. For this reason, in order to compare the thermal properties of other nanocomposites which prepared with

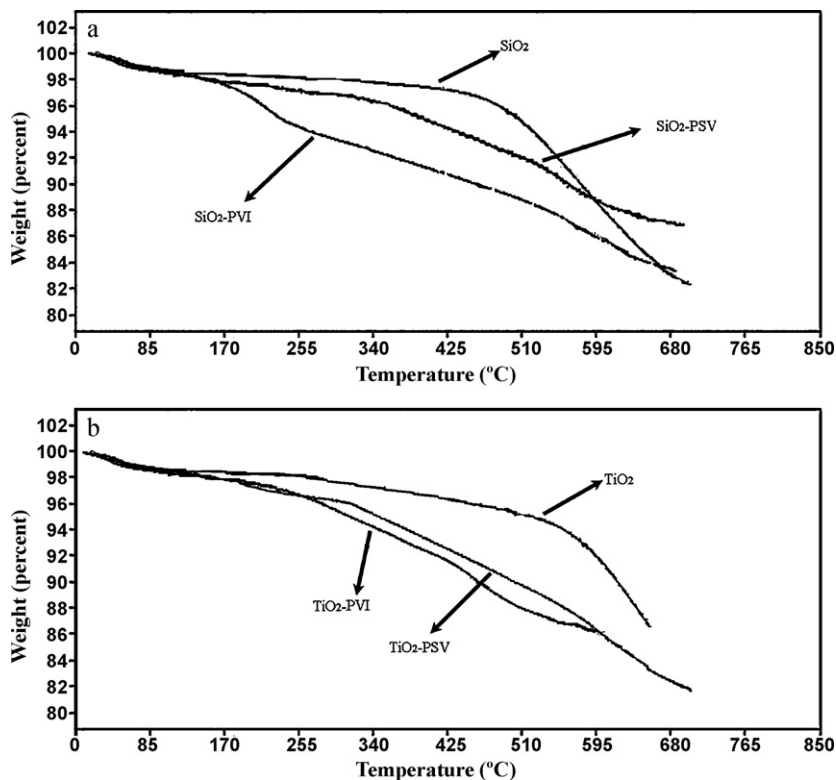


Fig. 5. TGA thermograms of modified and un-modified a) SiO_2 and b) TiO_2 .

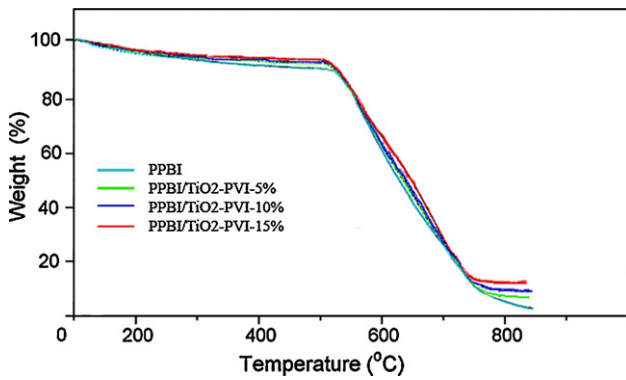


Fig. 6. The TGA thermograms of PPBI/TiO₂-PVI-5%, 10% and 15% nanocomposites.

modified nanoparticles having different monomers, only the TGA thermograms of nanocomposite containing of 10% (between 5% and 15%) modified nanoparticles are reported.

The remaining weight percentage in 850 °C is related to the modified TiO₂ that is less than the added amount of PVI-modified TiO₂ nanoparticles when the membrane was prepared. This decrease in weight in comparison with the theoretical amount could be related due to the degradation of the chains grafted onto the surface of the nanoparticles. Also, in order to obtain the particular weight of the modified nanoparticles, specific amounts of modified and un-modified nanoparticles were weighed after and before complete burning out all the polymers. They were heated to temperatures about 1000 °C for 30 min and the obtained nanoparticles were weighed immediately. The difference between the weight of un-modified nanoparticles before and after heating shows the amount of lost water which was either physically adsorbed or produced from the condensation reaction of the hydroxyl groups on the nanoparticle surface. Also from the difference between the weight of modified nanoparticles before and after heating and consider-

Table 1
The percentages values of grafted chains in nanoparticle surface.

Samples	Theoretical values (%)	Experimental values (%)
SiO ₂ -PVI	38	28
SiO ₂ -PSV	36	24
TiO ₂ -PVI	25	20
TiO ₂ -PSV	25	18

ing the weight of lost water, the percentage of the grafted polymer onto the nanoparticle surface was obtained. The obtained results and theoretical amounts are shown in Table 1. The amounts of the obtained results in all cases are more than theoretical values. This could be related to the presence of free water molecules and hydroxyl groups on the nanoparticles surface in which their values are not subtracted from theoretical values.

The diagrams of thermogravimetric analysis of both PPBI and nanocomposites prepared from the modified nanoparticles (10% w/w) are shown in Fig. 7. The weight loss observed in the temperature range of 50–140 °C is a result of the release of water adsorbed into the membranes which is less significant in nanocomposites in comparison to pure membrane.

The second loss in weight, observed at the temperature range of 500–530 °C, is also attributed to the thermal degradation of polymeric backbone of the nanocomposite membranes which is almost identical to the degradation temperature of pure PPBI. As a result, the addition of both modified and un-modified nanoparticles do not have any noticeable effect on thermal stability of the prepared nanocomposites.

As it is observed in Fig. 7, the degradation of PVI-modified nanoparticles occurs at 185 °C which is lower than the related temperature of PSV-modified ones. Therefore, the former one can be used in fuel cells with performance under 150 °C, but PSV-modified membrane is more suitable in high temperature fuel cells.

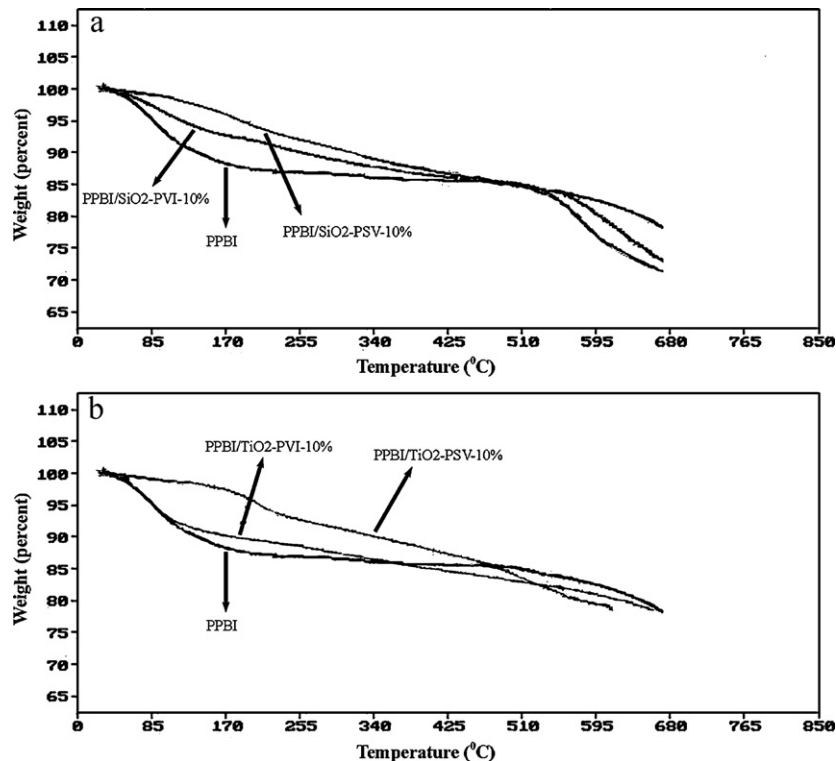


Fig. 7. TGA thermograms of PPBI and PPBI based nanocomposite membranes with modified a) SiO₂ and b) TiO₂ nanoparticles.

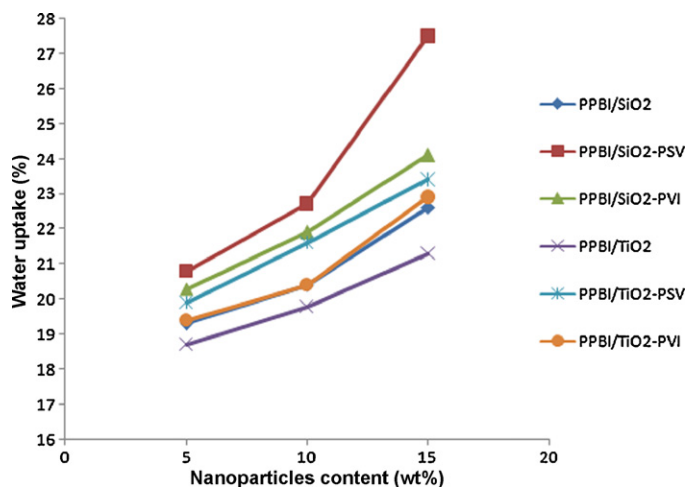


Fig. 8. Water uptake of nanocomposite membranes as a function of contents of nanoparticles.

3.3. Water uptake and doping level

Water uptake amount of nanocomposite membranes containing 5, 10 and 15% of modified nanoparticles at 25 °C are shown in Fig. 8. Addition of silica nanoparticles to PPBI membranes increased their water uptakes due to the hygroscopic nature of SiO₂ and TiO₂ nanoparticles. The sulfonic and imidazole groups in the nanoparticles increased the water uptake to a greater extent. The amount of water uptake for PPBI/TiO₂-PSV, PPBI/SiO₂-PSV, PPBI/TiO₂-PVI and PPBI/SiO₂-PVI are 21.6, 22.7, 20.4 and 21.9%, respectively. The effect of sulfonic acid groups of PSV chains grafted onto the nanoparticle surface on the water uptake is more than imidazole groups in PVI chains due to the higher hygroscopic properties of PSV comparing to PVI chains grafted on to the silica nanoparticle surface. The water uptake of PPBI/SiO₂-PSV is higher than PPBI/TiO₂-PSV which can be due to the further increase of the surface of SiO₂ nanoparticles in comparison to TiO₂ nanoparticle surface.

The PPBI-based membranes were doped with 85% H₃PO₄ to prepare the acid-doped membranes. Fig. 9 shows the acid-doping levels of the PPBI-based nanocomposite membranes. Acid-doping level (H₃PO₄ molecules per PPBI repeating unit) of pristine PPBI membrane was 13.5, which decreased to 11.8 for PPBI/SiO₂, 12.0 for PPBI/SiO₂-PSV, 11.7 for PPBI/TiO₂ and 12.2 for PPBI/TiO₂-PSV

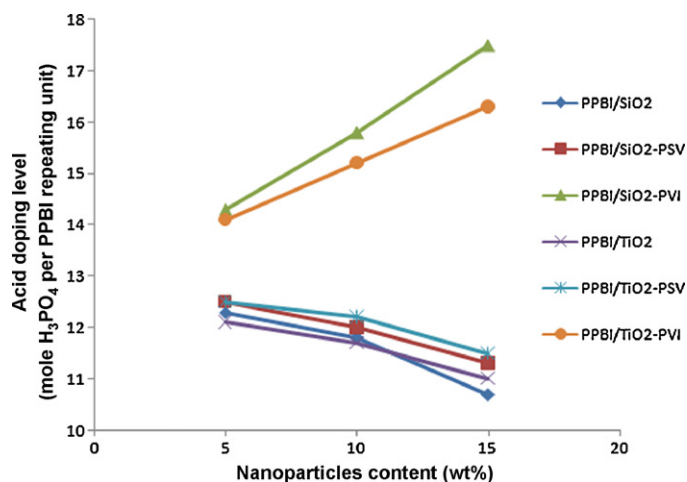


Fig. 9. Acid-doping levels of PPBI nanocomposite membranes as a function of contents of nanoparticles.

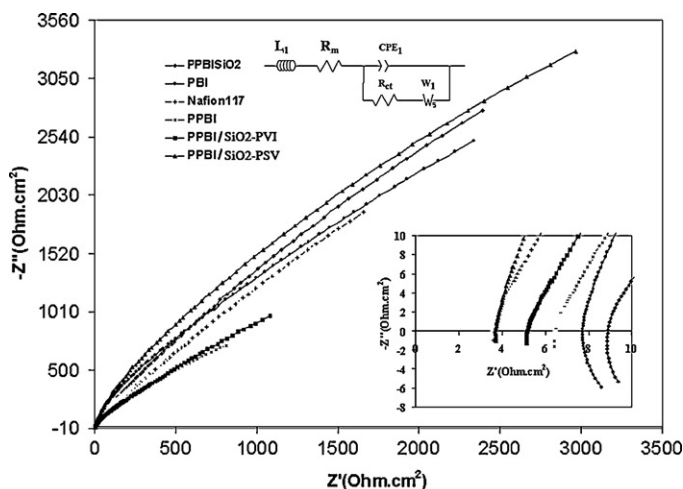


Fig. 10. The Nyquist plot of EIS data for nanocomposite membranes.

with 10% nanoparticle content and increased to 15.8 for PPBI/SiO₂-PVI and 15.2 for PPBI/TiO₂-PVI. Some of the amino groups in PPBI chains were blocked with the sulfonic acid groups of TiO₂-PSV and SiO₂-PSV, to decrease the binding ability of PPBI chains to H₃PO₄ molecules.

Among the prepared nanocomposites, the water uptake in PPBI/SiO₂-PSV and acid doping in PPBI/SiO₂-PVI were the most one. Even in the comparison of these membranes with the similar ones which prepared from modified TiO₂ such as PPBI/TiO₂-PSV and PPBI/TiO₂-PVI, the amount of water uptake and doping level were higher. This shows that using modified SiO₂ nanoparticles in fuel cells is more appropriate.

3.4. Proton conductivity

The membrane was sandwiched between two stainless steel electrodes and pressed together by clamp. Then, the MEA (Membrane Electrolyte Assembly) was inputted in the steam autoclave equipped with temperature controller. For measurement of proton conductivity, the steam autoclave supplied with steam from a house generator for exposure to saturated steam at desired temperature. As an example, for saturated steam the pressure corresponding to 120 °C is 205 kPa. The time of exposure to saturated steam at 120 °C was 30 min that this value for temperature of 140 °C was increased to 50 min.

Fig. 10 shows the Nyquist plot and equivalent circuit of studied membranes at 25 °C and RH 100% for some membranes.

After fitting the EIS experimental data on the electrical equivalent circuit, the membrane proton conductivity was determined from the intercept of EIS data with real impedance Z' axis (as the value of R_m element). In equivalent circuit, R_m presents the resistance of the polymer film between the two metallic electrodes toward charge carriers (i.e. H⁺). L_1 presents the stray inductance of the setup wires. CPE1 presents the non-ideal double layer capacitance of the film/metal electrode interface. R_{ct} and W_0 show the charge transfer resistance of the (possible) reactions at the film/metal electrode interface and the diffusion processes through the polymers film, respectively. The proton conductivities of the phosphoric acid-doped PPBI based nanocomposite membranes containing SiO₂ and TiO₂ (Fig. 11) at 100% relative humidity were presented as a function of temperatures up to 80 °C. The proton conductivities of all membranes increased with increasing the operation temperature up to 80 °C. Addition of the un-modified nanoparticles showed a negative effect on the proton conductivities of nanocomposite membranes. Similar trends were also reported to

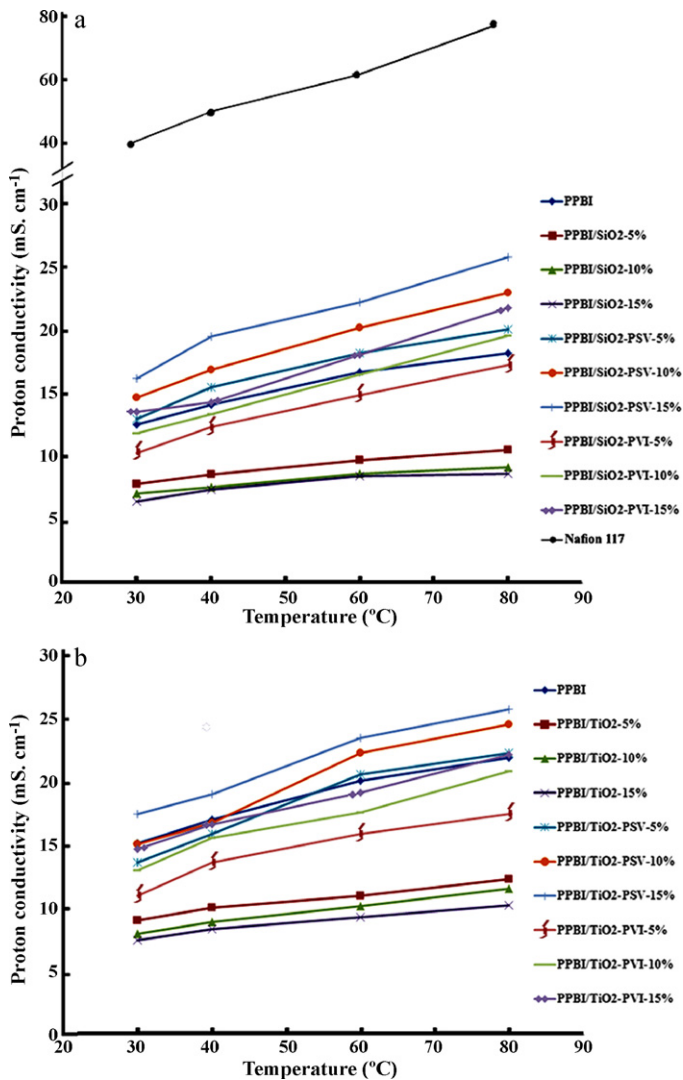


Fig. 11. Proton conductivities of PPBI based nanocomposite membranes containing SiO₂ (a) and TiO₂ (b) nanoparticles at 100% relative humidity up to 80 °C.

other nanocomposite membranes like Nafion[®]/silica membranes and PBI/silica membranes [31].

On the other hand, comparing the pristine PPBI and Nafion[®] 117 membranes, the relatively high proton conductivities of the nanocomposite membranes prepared from modified nanoparticles are noteworthy [32]. Li et al. have used sulfonated organosilica to modify Nafion[®] membranes and they found that the proton conductivities of the modified membranes were still lower than that of the neat Nafion[®] membrane.

The reduction in the proton conductivity was attributed to the silica-induced changes in the tortuous paths and in the distribution of hydrophilic/hydrophobic domains. However, in this work an enhancing effect on the proton conductivity was observed with addition of PSV and PVI grafted nanoparticles to PPBI membrane. The sulfonic and imidazole groups of modified nanoparticles also contribute in the acid-doping effect to PPBI polymer so as to enhance the proton conductivity of nanocomposite membranes prepared from modified nanoparticles. Moreover, the presence of modified nanoparticles induces proton conductive pathways leading to an increase in the proton conductivities of PPBI/modified nanoparticles membranes [24].

The proton conductivities of the acid-doped nanocomposite membranes containing SiO₂ and TiO₂ (Fig. 12) were further

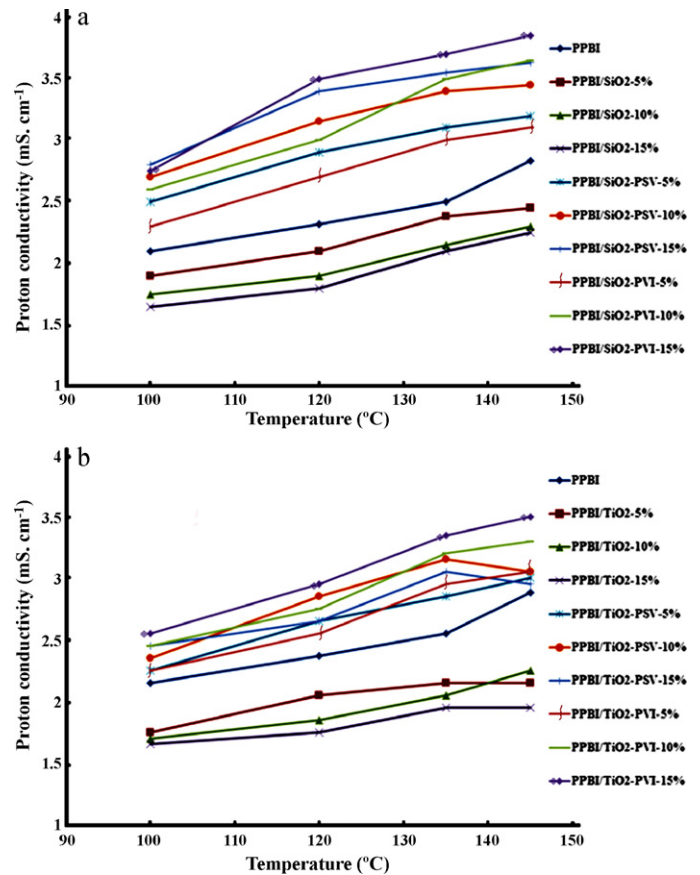


Fig. 12. Proton conductivities of PPBI based nanocomposite membranes containing SiO₂ (a) and TiO₂ (b) nanoparticles at dry environment up to 145 °C.

studied at high temperatures under an anhydrous environment. All the PPBI/modified nanoparticle membranes still exhibited higher proton conductivities than the pristine acid-doped PPBI membrane.

Generally, two principle mechanisms of vehicle mechanism and Grotthuss mechanism (hopping) describe proton diffusion through the membrane [33]. It is possible that the bounded water participates by the Grotthuss mechanism, and the free water takes part mostly by vehicle mechanism [34]. Addition of silica-SO₃H to the membranes increases the bounded water content in the membranes (Fig. 13). The bounded water facilitates the proton transport ability through the Grotthuss mechanism, originating by generation of a continuous proton conductive pathway. Therefore, the high proton conductivity of PPBI/modified nanoparticles can be attributed to the high bounded water content in the membrane.

Since the Grotthuss-type diffusion mechanism without assistance of the vehicle mechanism has been proposed for the proton conduction under anhydrous environments [35,36], the proton conductivity of the acid-doped PPBI/modified nanoparticle membranes could be synergistically resulted from their modified nanoparticle contents and the acid-doping levels.

Consequently, the highest proton conductivity was obtained with the acid-doped PPBI/SiO₂-PSV-15% membrane at high humidity and low temperatures and PPBI/SiO₂-PVI-15% membrane in high temperatures and low humidity, which possesses the moderate modified nanoparticles content and acid-doping level.

As it is seen in Fig. 9, either we use PSV-modified or un-modified nanoparticles, the increase in the amount of the nanoparticles leads

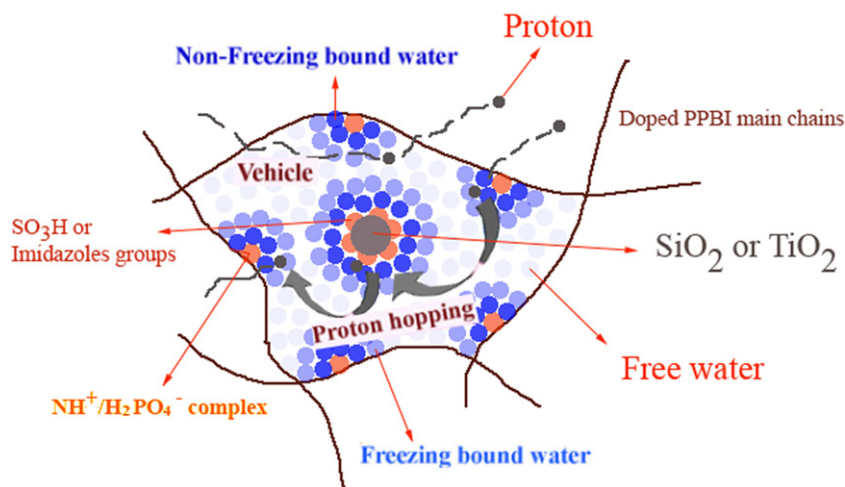


Fig. 13. Illustration of the state of water in the membranes, the interaction between the functional groups of nanoparticles and of PPBI to restrict the nanoparticles motion, and the proton-transport mechanism in the membranes [24].

to a decrease in the acid doping level, but when PVI-modified nanoparticles were used, doping level increased. Also, according to Fig. 8, water uptake of the membrane shows an increase when using higher amounts of modified nanoparticles. This increase in PSV-modified nanocomposite membranes is higher in PVI-modified one. Proton conductivity of the nanocomposite membranes obtained from PSV-modified nanoparticles shows significant increase in comparison to PVI-modified ones in low temperature and high relative humidity. But in high temperature and low relative humidity, proton conductivity of the nanocomposite membranes obtained from PVI-modified nanoparticles is observed to be more than PSV-modified ones and even at 145 °C the proton conductivity of PPBI/SiO₂-PVI 15% is more than PPBI/SiO₂-PSV-15%. The existence of modified nanoparticles in PPBI nanocomposite membranes results in high proton conductivity in three ways:

- 1) With increase in water uptake
- 2) With increase in the amount of doping level and
- 3) With increase in the number of proton conductive functional groups such as sulfonic acid group.

In PSV-modified nanocomposite membranes, acid doping decreases while the water uptake and the number of sulfonic acid groups shows an increase. Consequently, high proton conductivity can be a result of these changes. It should be mentioned that in temperatures higher than 100 °C and in very low relative humidity, water uptake of PSV-modified membranes decreases which leads to low efficiency of the sulfonic groups attached onto the surface of the nanoparticles which in turn results in a decrease in proton conductivity in both membranes, but the increase in proton conductivity resulting from high doping level is significant and also the proton conductivity of PVI-modified nanocomposite membranes increase in high temperatures.

It is noteworthy that Nafion[®] 117 shows relatively low proton conductivities under anhydrous conditions and almost lacks its proton conductivities at high temperatures. Comparing to Nafion[®] 117 membranes, the high proton conductivities of PBI/SiO₂-PVI 10% indicate that this membrane could be utilized as proton exchange membranes for fuel cell at high temperatures and dry conditions.

3.5. Mechanical properties

The mechanical properties of the PPBI-based membranes were measured. The stress–strain curves are shown in Fig. 14. Pristine

PPBI membrane showed an elongation at break of 38%. Modification of nanocomposites with SiO₂ and TiO₂ nanoparticles results in an increase in the tensile strengths and a subsequent decrease in the elongations at break for the PPBI-based membranes. For PPBI/modified nanoparticles nanocomposites membranes (PPBI/modified nanocomposite consists of the PPBI and surface-modified SiO₂ and TiO₂ nanoparticles by PVI and PSV chains and PPBI/unmodified nanocomposite includes PPBI and SiO₂ and TiO₂ nanoparticles without any treatment), the presence of ionic linkages between PPBI and silica particles can be assigned to their high Young's modulus. Introduction of modified and un-modified nanoparticles increases the brittleness of the nanocomposite membranes with a decrease in their elongations at break. The effects of modified and unmodified nanoparticles on the elongations at break of the nanocomposite membranes were different. The decrease in the elongation at break and increase in the brittleness were widely observed with polymer nanocomposites and could be attributed to the presence of inorganic reinforcement [37–39]. Moreover, the ionic linkages in nanocomposite membranes prepared from modified nanoparticles are higher than hydrogen bonding in PPBI/SiO₂ and PPBI/TiO₂.

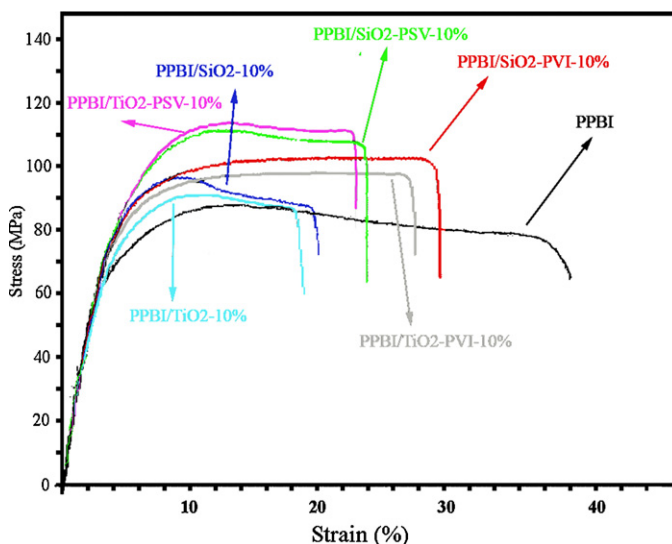


Fig. 14. Stress–strain curves of PPBI and nanocomposite membranes containing 10% nanoparticles.

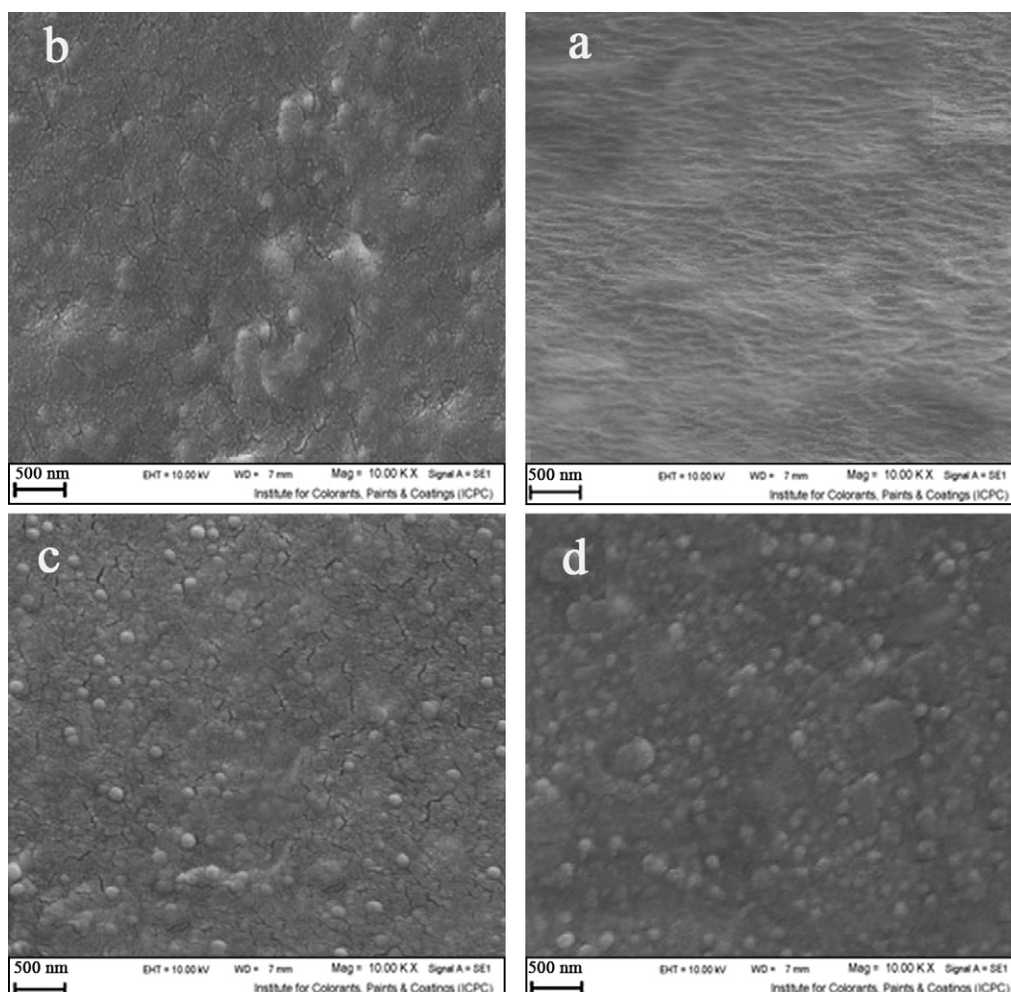


Fig. 15. The SEM photograph of a) pure PPBI membrane and TiO_2 -PSV nanocomposite membranes containing of b) 5%, c) 10% and d) 15% nanoparticles.

The brittleness of PPBI/ TiO_2 based nanocomposite membranes is higher than PPBI/ SiO_2 ones. The brittleness of membranes prepared from TiO_2 -PVI and SiO_2 -PVI are less than PPBI/ SiO_2 -PSV and PPBI/ TiO_2 -PSV membranes which are perhaps due to more compatibility of PVI grafted chains onto the nanoparticles surface with PPBI backbone.

Comparing the brittleness of the nanocomposite membranes of the PPBI/ SiO_2 -PSV and PPBI/ SiO_2 -PVI with PPBI/ TiO_2 -PSV and PPBI/ TiO_2 -PVI, respectively indicates that the brittleness of the membranes prepared with modified SiO_2 nanoparticles is less than the modified TiO_2 ones.

3.6. Morphological analysis

The scanning electron microscopy (SEM) photographs of the PPBI/ TiO_2 -PSV nanocomposite membranes surface with various amounts of TiO_2 -PSV are shown in Fig. 15.

A relatively flat surface is observed for thin membranes of pure PPBI (Fig. 15(a)). Fig. 15(b–d) display surface morphological properties of nanocomposite membranes having 5, 10 and 15% of TiO_2 -PSV, respectively.

As seen in Fig. 15, TiO_2 -PSV nanoparticles are dispersed homogeneously in PPBI matrixes and are increased with increasing of the percentage of TiO_2 -PSV nanoparticles. Also the major amounts of nanoparticles size are in the range of nanoscale and the bigger particles as evidence for the formation of aggregations are not observed.

The size of the TiO_2 -PSV particles are about 25–40 nm and the size of particles on the surface of the nanocomposite are determined to be 30–60 nm.

Fig. 16(a) shows the SEM micrographs of the modified SiO_2 nanoparticles. If the interactions between silica nanoparticles are stronger than that of between PPBI molecules and silica nanoparticles, the silica nanoparticles are agglomerated together to form silica domains in micrometer sizes. The compatibility between PPBI and unmodified nanoparticles and the homogeneity of the PPBI/ SiO_2 or PPBI/ TiO_2 membranes are somewhat poor [32].

However, the dispersion homogeneity of silica nanoparticles in PPBI membranes could be significantly improved with using surface modified nanoparticles as the additives. As shown in Fig. 16(b), the dispersion homogeneity of modified nanoparticles is observed in the TEM micrograph of PPBI/PSV- SiO_2 nanocomposite membrane, which demonstrates high compatibility between PPBI polymer and PSV- SiO_2 nanoparticles and the high dispersion ability of PSV- SiO_2 in PPBI matrix. Particle agglomeration is still not observed in the TEM micrograph of PPBI/PSV- SiO_2 -10%. The ionic linkages between PPBI and modified nanoparticles are contributed to their higher compatibility [32]. However, in nanocomposite membranes prepared from un-modified SiO_2 nanoparticles, the dispersion of the nanoparticles in polymer matrix is not homogenous and probably aggregation has been formed (Fig. 16(c)).

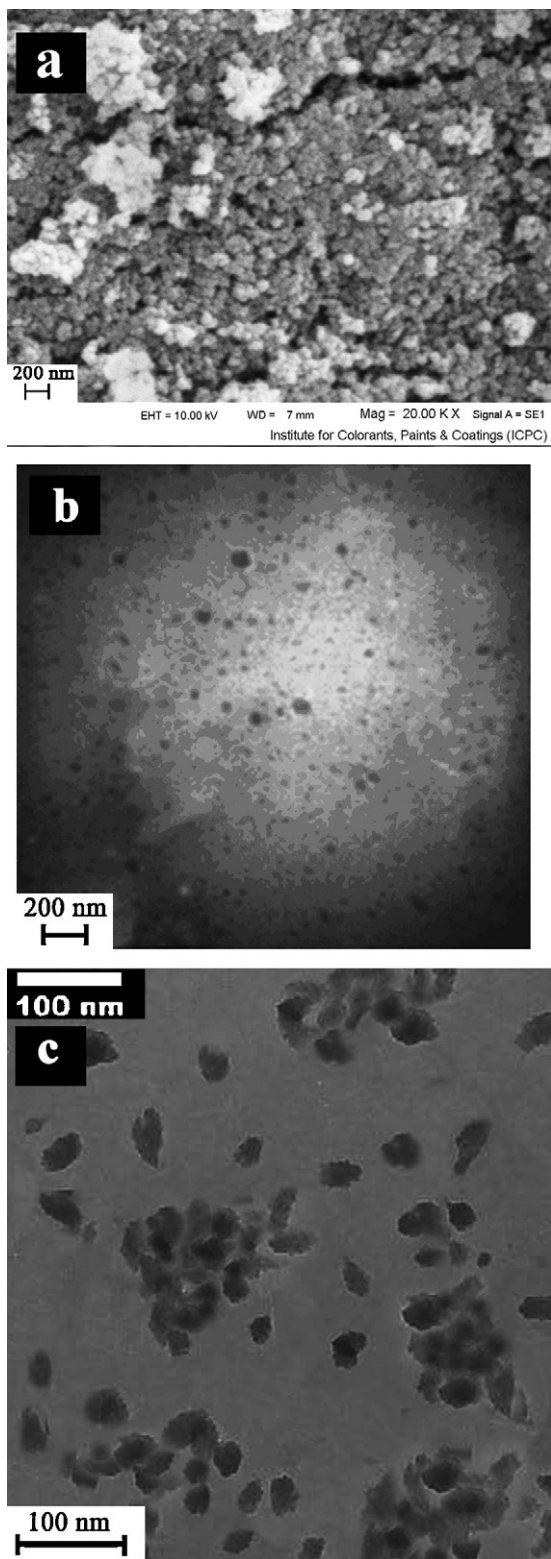


Fig. 16. SEM micrograph of SiO₂-PSV (a); TEM micrographs of PPBI/SiO₂-PSV-10% (b); and PPBI/SiO₂-10% (c).

4. Conclusion

The nanocomposite PPBI-based membranes were prepared using various amounts of modified and un-modified TiO₂ and SiO₂ nanoparticles. The thermal stability of the prepared nanocompos-

ite membranes was similar to PPBI membrane. The water uptake of the nanocomposite membranes prepared from TiO₂/PSV and SiO₂/PSV nanoparticles were higher than other nanocomposite membranes. The acid doping level and proton conductivity of the nanocomposite membranes in dry conditions obtained from TiO₂-PVI and SiO₂-PVI nanoparticles were the highest in comparison to PPBI/SiO₂-PSV and PPBI/TiO₂-PSV. Formation of nanocomposites with modified and un-modified nanoparticles resulted the increasing of tensile strengths. The decreasing in the elongation at break and increase in the brittleness was widely observed with polymer nanocomposites and could be attributed to the presence of inorganic reinforcement. The high proton conductivities of PBI/SiO₂-PVI 10% indicated that this membrane could be utilized as a proton exchange membrane for fuel cell at high temperatures and dry conditions.

Acknowledgments

The authors would like to acknowledge Dr. M.-G. Hosseini and I. Ahadzadeh for proton conductivity measurements, Ms. M. Namvari for English editing and the University of Tabriz for financial supports of this project.

References

- [1] A. Saccà, A. Carbone, E. Passalacqua, A. D'Epifanio, S. Licocchia, E. Traversa, E. Sala, F. Traini, R. Ornelas, J. Power Sources 152 (2005) 16–21.
- [2] A. Saccà, I. Gatto, A. Carbone, R. Pedicini, E. Passalacqua, J. Power Sources 163 (2006) 47–51.
- [3] I. Gatto, A. Saccà, A. Carbone, R. Pedicini, F. Urbani, E. Passalacqua, J. Power Sources 171 (2007) 540–545.
- [4] F. Lufrano, I. Gatto, P. Staiti, B. Antonucci, E. Passalacqua, Solid State Ionics 145 (2001) 47–51.
- [5] J. Kerres, A. Ullrich, F. Meier, Th. Haring, Solid State Ionics 125 (1999) 243–249.
- [6] A. Carbone, R. Pedicini, G. Portale, A. Longo, L. D'Ilario, E. Passalacqua, J. Power Sources 163 (2006) 18–26.
- [7] R.J. Spry, M.D. Alexander Jr., S.J. Bai, T.D. Dang, G.E. Price, D.R. Dean, B. Kumar, J.S. Solomon, F.E. Arnold, J. Polym. Sci., Part B: Polym. Phys. 35 (1997) 2925–2933.
- [8] P. Staiti, F. Lufrano, A.S. Aricò, E. Passalacqua, V. Antonucci, J. Membr. Sci. 188 (2001) 71–78.
- [9] J.M. Bae, I. Honma, M. Murata, T. Yamamoto, M. Rikukawa, N. Ogata, Solid State Ionics 147 (2002) 189–194.
- [10] D.J. Jones, J. Rozière, J. Membr. Sci. 185 (2001) 41–58.
- [11] J. Labato, P. Canizares, M.A. Rodrigo, J.J. Linares, G. Manjavacas, J. Membr. Sci. 280 (2006) 351–362.
- [12] H.-J. Kim, S.J. An, J.-Y. Kim, J.K. Moon, S.Y. Cho, Y.C. Eun, H.-K. Yoon, Y. Park, H.-J. Kweon, E.-M. Shin, Macromol. Rapid Commun. 25 (2004) 1410–1413.
- [13] Q. Li, H.A. Hjuler, N.J. Bjerrum, J. Appl. Electrochem. 31 (2001) 773–779.
- [14] M. Watanabe, H. Uchida, Y. Seki, M. Emori, P. Stonehart, J. Electrochem. Soc. 143 (1996) 3847–3852.
- [15] M. Watanabe, H. Uchida, M. Emori, J. Electrochem. Soc. 145 (1998) 1137–1141.
- [16] P.L. Antonucci, A.S. Arico, P. Creti, E. Ramunni, V. Antonucci, Solid State Ionics 125 (1999) 431–437.
- [17] K.T. Adjemian, S.J. Lee, S. Srinivasan, J. Benziger, A.B. Bocarsly, J. Electrochem. Soc. 149 (2002) A256–A261.
- [18] V. Baglio, A.D. Blasi, A.S. Aricò, V. Antonucci, P.L. Antonucci, F. Serraino Fiory, S. Licocchia, E. Traversa, J. New Mater. Electrochem. Syst. 7 (2004) 275–280.
- [19] D.C. Hague, M.J. Mayo, J. Am. Ceram. Soc. 77 (1994) 1957–1960.
- [20] A. Carbone, R. Pedicini, A. Saccà, I. Gatto, E. Passalacqua, J. Power Sources 178 (2008) 661–666.
- [21] A. Carbone, A. Saccà, I. Gatto, R. Pedicini, E. Passalacqua, Int. J. Hydrogen Energy 33 (2008) 3153–3158.
- [22] C.H. Rhee, H.K. Kim, H. Chang, J.S. Lee, Chem. Mater. 17 (2005) 1691–1697.
- [23] P. Bébin, M. Caravanier, H. Galiano, J. Membr. Sci. 278 (2006) 35–42.
- [24] Y.H. Su, Y.L. Liu, Y.M. Sun, J.Y. Lai, D.M. Wang, Y. Gao, B. Liu, M.D. Guiver, J. Membr. Sci. 296 (2007) 21–28.
- [25] P. Staiti, Mater. Lett. 47 (2001) 241–246.
- [26] P. Staiti, M. Minutoli, S. Hocevar, J. Power Sources 90 (2000) 231–235.
- [27] E.B. Easton, Z. Qi, A. Kaufman, P.G. Pickup, Electrochem. Solid-State Lett. 4 (2001) A59–A61.
- [28] A. Wanda, P. Peter, J. Solid State Electrochem. 8 (2004) 742–747 (6).
- [29] B. Christele, B. Emmanuel, B. Elodie, C. Philippe, Z. Nathalie, Polymer 46 (2005) 8502–8510.
- [30] D.S. Kim, G.P. Robertson, M.D. Guiver, Macromolecules 41 (2008) 2126–2134.
- [31] C.N. Li, G.Q. Sun, S.Z. Ren, J. Liu, Q. Wang, Z.M. Wu, H. Sun, W. Jin, J. Membr. Sci. 272 (2006) 50–57.
- [32] Suryani, Y.-L. Liu, J. Membr. Sci. 332 (2009) 121–128.

- [33] K.D. Kreuer, Chem. Mater. 8 (1996) 610–641.
- [34] D.S. Kim, B. Liu, M.D. Guiver, Polymer 47 (2006) 7871–7880.
- [35] Y.L. Ma, J.S. Wainright, M.H. Litt, R.F. Savinell, J. Electrochem. Soc. 151 (2004) A8–A16.
- [36] R. He, Q. Li, J.O. Jensen, N.J. Bjerrum, J. Polym. Sci., Part A: Polym. Chem. 45 (2007) 2989–2997.
- [37] S.Md. Mominul Alam, T. Agag, T. Kawauchi, T. Takeichi, React. Funct. Polym. 67 (2007) 1218–1224.
- [38] G. Ramorino, F. Bignotti, S. Pandini, T. Riccò, Compos. Sci. Technol. 69 (2009) 1206–1211.
- [39] C. Parka, J.G. Smith Jr., J.W. Connell, S.E. Lowtherb, D.C. Working, E.J. Siochi, Polymer 46 (2005) 9694–9701.